Simultaneous Description of Positive and Negative Parity Bands in even-even and even-odd Nuclei

Article · January 2011

1 author:

Apolodor Raduta
Horia Hulubei National Institute for R&D in Physics and Nuclear Engineering
307 PUBLICATIONS **2,333** CITATIONS

SEE PROFILE

SIMULTANEOUS DESCRIPTION OF POSITIVE AND NEGATIVE PARITY BANDS IN EVEN-EVEN AND EVEN-ODD NUCLEI

A. A. RADUTA[a),b)] and C. M. RADUTA [a)]

[a)] Department of Theoretical Physics, IFIN-HH, Bucharest, POBox MG6, Romania

[b)] Academy of Romanian Scientists, 54 Splaiul Independentei, Bucharest 050094, Romania

A unified description of four positive and four negative parity rotational bands for even-even nuclei with and without octupole deformation is presented within an extended version of the coherent state model. Signatures for octupole deformation in the ground as well as in the excited bands are pointed out. Specific features of octupole deformed nuclei related with the electric and magnetic transition probabilities are presented. The second part of the present lecture regards the parity partner bands in even-odd nuclei. Comments about a possible chiral symmetry to be detected in odd nuclear systems are added. To save the space, only part of the applications performed in the last decade were reviewed.

I. INTRODUCTION

Low-lying negative parity states were first observed in Ra and Th nuclei by high-resolution alpha spectroscopy measurements by Asaro et al. in 1953 [1] and Stephen et al. in 1955 [2]. Indeed, by angular correlations and gamma coincidence a spin sequence $1, 3, 5, ...$ of negative parity has been identified. The states were interpreted as describing vibrations around a spherical equilibrium shape. Microscopically, such vibrations are caused by particle-hole (ph) excitations induced by octupole-octupole two body interaction. Long time people thought that the negative parity states are similar with the vibrational states of positive parity, the only difference being the parity. The interest for negative parity states increased dramatically when two theoretical works predicted that some nuclei might have a static octupole deformation. Indeed, in Ref.[3] Chasman predicted parity doublets for several odd mass isotopes of Ac, Th, and Pa. The doublet members have the same angular momentum, different parities, large connecting E3 transition and almost the same energy. The parity doublet of lowest energy plays the role of a degenerate ground state with a broken parity reflection-symmetry. Advancing the parity doublet hypothesis, Chasman was able

to describe consistently the data in the nuclei mentioned above. In the second paper [4], Moller and Nix showed that the binding energy in the mass region of 224 gains about 1.5 MeV when the octupole deformation is included in the mean field of the potential energy.

By contrast to the case of nuclei having only quadrupole deformation, a nuclear surface with a static octupole deformation does not exhibit a space reflection symmetry. On the other hand breaking a symmetry leads to setting on a new nuclear phase, with specific properties. Therefore, one expects that an octupole deformed nucleus has properties which are not met in nuclei with good space reflection symmetry. Due to this feature the study of the rotational bands in octupole deformed nuclei is of a paramount importance. However, it is difficult to identify the nuclei with a static octupole deformation. The reason is that there is no measurable observable which may quantitatively describe the octupole deformation. Therefore, information about it should be indirectly obtained from energy levels.

In the framework of microscopic theories the onset of octupole deformation is caused by the octupole interaction of orbits lying close to the Fermi sea and characterized by $\Delta j = \Delta l = 3$. In this context the octupole deformed nuclei should have the Fermi level close to the intruder state. Low lying negative parity states (nps) are compatible only with a potential energy exhibiting a flat deformed minimum. This means that a nucleus with a low lying negative parity state may be suspected to have a static octupole deformation. Along the time several signatures for octupole deformation have been pointed out. Here is the list of properties considered to be signatures for a static octupole deformation.

- In the even-even pear shape nuclei the negative and positive parity states (belonging to the ground band) form an alternating parity spectrum with a parity doublet structure.
- The two interleaved bands show an identical J(J+1) pattern, i.e. rotations in the two bands are characterized by identical moments of inertia.
- The negative parity members of doublets have enhanced E1 rates and moments.
- The experimental data show that the hindrance factor for an alpha decay from a state of a given parity to the doublet member of opposite parity is enhanced by 2-3 orders of magnitude.

Contributions to the description of various properties of the octupole deformed nuclei have been reviewed in several papers [5, 6]. Due to the space restriction we confine our review to the contri-

butions performed with a single formalism, namely the one which is able to describe in a consistent manner a large volume of data.

Thus the aim of our lecture is to investigate some properties of octupole bands within a formalism which represents an extension [7–11, 13] of the coherent state model (CSM)[14]. Our intentions regard the following features: i) The interleaved structure in the g, β and γ bands for some even-even isotopes of Ra, Th, U, Pu, Gd, Yb. ii) The low excitation energy for the state 1^- in ^{218}Ra. iii)The description of the E1 branching ratios. iv) Are there signatures for static octupole deformation in the excited bands? v) What are the specific properties for the dipole bands. vi) Could an octupole deformed nucleus have a chiral symmetry? In the second part of my talk the formalism is extended to the even-odd systems. Results are shown for few isotopes and concerns the bands with $K^\pi = \frac{1}{2}^\pm, \frac{3}{2}^\pm, \frac{5}{2}^\pm$.For these bands some relevant data concerning the transition probabilities are given. Possible signatures for static octupole deformation and chiral symmetry in the odd systems are investigated.

II. SIMULTANEOUS DESCRIPTION OF FOUR POSITIVE AND FOUR NEGATIVE PARITY BANDS IN SOM EVEN-EVEN ISOTOPES

A. Brief review of CSM

The intrinsic deformed states modeling the ground, beta and gamma bands must satisfy a set of restrictions suggested by the experimental data. These restrictions have been formulated in Ref.[14] and in brief they are: a) the states are deformed functions of quadrupole bosons, $b^\dagger_{2\mu}$; b) the states in the laboratory frame are obtained through an angular momentum projection procedure; c) the states are orthogonal before and after angular momentum projection; d) functions depend on a real parameter simulating the quadrupole deformation; e) in the vibrational region the functions describe a degenerate multi-boson state while in the large deformation regime they are proportional to a Wigner function of a definite K; f) the link between the vibrational and rotational functions is achieved in full agreement with the Sheline-Sakai scheme[15, 16]; g) the projected states span a restricted collective space where an effective Hamiltonian is constructed. In Ref.[14] we found a solution for the deformed states obeying these criteria.

The projected states defining the ground, beta and gamma bands , are:

$$\varphi^{(i)}_{JM} = N^{(i)}_J P^J_{MK_i} \Phi_i, i = g, \beta, \gamma \tag{2.1}$$

where the projection operator is defined by:

$$P^J_{MK} = \frac{2J+1}{8\pi^2} \int d\Omega D^{J^*}_{MK}(\Omega) R(\Omega), \tag{2.2}$$

and acts on intrinsic mutually orthogonal states of the form

$$\begin{aligned}
\Phi_g &= exp\left[d\left(b^+_{20} - b_{20}\right)\right]|0>_{(2)} \ , \\
\Phi_\beta &= \Omega^\dagger_\beta \Phi_g \\
&\equiv \left[\left(b^\dagger_2 b^\dagger_2 b^\dagger_2\right)_{00} + \frac{3}{\sqrt{14}}\, d\left(b^\dagger_2 b^\dagger_2\right)_{00} - \frac{d^3}{\sqrt{70}}\right]\Phi_g \ , \\
\Phi_\gamma &= \Omega^\dagger_\gamma \Phi_g \equiv \left[\left(b^\dagger_2 b^\dagger_2\right)_{22} + \sqrt{\frac{2}{7}}\, d\ b^\dagger_{22}\right]\Phi_g \ .
\end{aligned} \tag{2.3}$$

It can be checked that these projected states are orthogonal. Also the un-projected states have this property. The parameter d is real and simulates the nuclear deformation.

An effective Hamiltonian is then constructed such that a maximal decoupling of the projected states is achieved

$$\hat{H}_2 = A_1\left(22\hat{N}_2 + 5\Omega^\dagger_{\beta'}\Omega_{\beta'}\right) + A_2\hat{J}^2_2 + A_3\Omega^\dagger_\beta\Omega_\beta \ , \tag{2.4}$$

$\hat{J}_2$ is the total angular momentum, $\hat{N}_2$ is the quadrupole boson number operator and

$$\Omega^\dagger_{\beta'} = (b^\dagger_2 b^\dagger_2)_0 - \frac{d^2}{\sqrt{5}}. \tag{2.5}$$

With this Hamiltonian all states of the beta band and those of the gamma band with odd J are completely decoupled. Only the states of the gamma band with even J are coupled to the ground band states of similar angular momentum. In this case, for a given J the energies are computed by diagonalizing the boson Hamiltonian in a two-dimensional space. The coupling is in any case vanishing in the vibrational and rotational limits and is small in the transitional regime. The CSM was successfully used to describe the g, β and γ states, including those of high spin, in the Pt, rare earth and actinide regions.

In order to enlarge the range of its applicability we proposed several independent CSM extensions: a) By adding the quasiparticle degrees of freedom the back-bending phenomena in even-even and even-odd nuclei could be studied [17, 18]. b) A distinction between protons and neutrons was made in order to allow for a description of the low-lying orbital $M1$ mode[19]. c) Three negative parity bands with $K^\pi = 0^-, 1^-, 2^-$ were described by exciting, with an octupole boson, the

g, β, γ bands given by the CSM model [20]. In this way the vibrational-negative parity bands were described.

To stress on the specific features, CSM has been extensively compared with others phenomenological models like: i) the liquid drop model (LD); ii) the rotation-vibration model (RVM); iii) the Interacting Boson Approximation (IBA). This latter study clearly shows that the two models differ in their basic conceptual assumptions and their range of applicability. Indeed, while IBA is not working for deformed nuclei as well as for the high spin states, the CSM works especially well under these circumstances due to its semiclassical character.

B. CSM extension to the negative parity states

We suppose that the ground state exhibits both quadrupole and octupole deformations and is described by a product of two coherent functions for quadrupole and octupole bosons, respectively [7]:

$$\Psi_g = e^{f(b_{30}^+ - b_{30})} e^{d(b_{20}^+ - b_{20})} |0\rangle_2 |0\rangle_3, \tag{2.6}$$

d and f are real parameters which simulate the quadrupole and octupole nuclear deformations, respectively. This function is a sum of two components with different parities $\Psi^{\pm}$ which define, through the angular momentum projection, two sets of states respectively:

$$\varphi_{JM}^{(g,k)} = N_J^{(g,k)} P_{M0}^J \Psi_g^{(k)}, \quad K = \pm \tag{2.7}$$

$$J = \delta_{k,+}(even) + \delta_{k,-}(odd). \tag{2.8}$$

The normalization factors have the expressions:

$$\left(N_J^{(g,k)}\right)^{-2} = e^{-\frac{1}{2}(2y_3+3y_2)}(2J+1)\mathcal{I}_{(g,J)}^{(k)}(y_2,y_3),\ y_2 = d^2, y_3 = f^2. \tag{2.9}$$

where the overlap integrals are given by:

$$\mathcal{I}_{(g,k)}^J = (3y_3)^J \sum_{p=p_{min}}^{\infty} \sum_{l=0}^{l_{Max}} \left(\frac{y_3^2}{4}\right)^{p-l} (9)^p \left(\frac{5}{27}\right)^l (-)^{l+J} \times \frac{(p+J)!(2p+J)!F(-l, 2p-3l+J+1; \frac{9}{10}y_2)}{l!p!(2p-3l+J)!(2p+2J+1)!}.$$

Alternatively, the projected states can be written in a tensorial form as:

$$\varphi_{JM}^{(g,k)} = \mathcal{N}_J^{(g,k)} \sum_{J_2,J_3} (N_{J_3}^{(k)} N_{J_2}^{(g)})^{-1} C_{0\ 0\ 0}^{J_3\ J_2\ J} [\Psi_{J_3}^{(k)} \varphi_{J_2}^{(g)}]_{JM}\ ;\quad k = \pm\ . \tag{2.10}$$

In this case all matrix elements for quadrupole operators can be expressed as simple functions of overlap integrals:

$$I_J^{(0)} = \int_0^1 P_J(x) e^{d^2 P_2(x)} dx, \tag{2.11}$$

and $I_J^{(1)}$, which is the first derivative of $I_J^{(0)}$ with respect to $y_2(= d^2)$. If the intrinsic ground state has not a good reflection symmetry it sounds reasonable to assume that intrinsic gamma and beta bands have also this property. Then instead of using Φ_γ and Φ_β as model states of the two bands we propose now to choose the following functions:

$$\Psi_\gamma = \Omega_\gamma^+ \Psi_g, \quad \Psi_\beta = \Omega_\beta^+ \Psi_g. \tag{2.12}$$

Projecting first the parity and then the angular momentum, one obtains four bands, two of positive and two of negative parity:

$$\varphi_{JM}^{(i,k)} = \mathcal{N}_J^{(i,k)} P_{MK_i}^J \Psi_i^{(k)} \quad ; i = \beta, \gamma \ \ ; \ k = \pm \ , \tag{2.13}$$

with

$$\begin{aligned} \Psi_i^{(\pm)} \ &= \ \Omega_i^+ e^{-\frac{y_3+y_2}{2}} \begin{pmatrix} cosh(f b_{30}^+) \\ sinh(f b_{30}^+) \end{pmatrix} e^{d b_{20}^+} \mid 0\rangle_3 |0\rangle_2 \ ; \\ i \ &= \ \beta, \gamma \ ; \ K_i = 2\delta_{i,\gamma}, \ y_2 = d^2, y_3 = f^2. \end{aligned}$$

These functions can be also written as superposition of products of quadrupole and octupole projected states.

$$\varphi_{JM}^{(i,k)} = \mathcal{N}_J^{(g,k)} \sum_{J_2,J_3} (N_{J_3}^{(k)} N_{J_2}^{(g)})^{-1} C_{0 \ 0 \ 0}^{J_3 \ J_2 \ J} [\Psi_{J_3}^{(k)} \varphi_{J_2}^{(i)}]_{JM}. \tag{2.14}$$

Since for large values of the deformation parameter d, the projected states $\varphi_{JM}^{(i)}$ with $i = g, \beta, \gamma$ behave like a Wigner function with a definite quantum number "K", they describe rotational bands with $K = 0, 0, 2$, respectively. Analogously, the octupole states $\Psi_{JM}^{(\pm)}$ describe rotational bands having $K = 0$. Consequently, four of the six bands defined above have $K = 0$, while the remaining two are $K = 2$ bands. In order to stress on the parity partnership, we use the suggestive notations $g^\pm, \beta^\pm, \gamma^\pm$ for the six bands. Each pair of bands is expected to give rise to an alternating parity sequence as it happens in the case of ground and $K^\pi = 0^-$ bands, i.e. the $g^\pm$ pair. The set $\{\varphi_{JM}^{(i,k)}\}_{i,k;J,M}$ with $i = g, \beta, \gamma$ and $k = \pm$ is orthogonal. Note that for $f = 0$ only the positive parity states $\varphi_{J_3 M_3}^{(+)}$ are well defined. However, the limits for "f" going to zero exist both for $k = +$ and $k = -$, and the following relation holds:

$$\lim_{f \to 0} \varphi_{JM}^{(i,+)} = \varphi_{JM}^{(i)}. \tag{2.15}$$

Thus, the formalism proposed yields the CSM in the limit of $f \to 0$. Following the CSM, we define a model Hamiltonian which is effective in the model space of projected states. The effectiveness criteria is satisfied by:

$$\begin{aligned}\hat{H} &= \hat{H}'_2 + \mathcal{B}_1\hat{N}_3(22\hat{N}_2 + 5\Omega^+_{\beta'}\Omega_{\beta'}) + \mathcal{B}_2\hat{N}_3\Omega^+_\beta\Omega_\beta \\ &+ \mathcal{B}_3\hat{N}_3 + \mathcal{A}_{(J23)}\,\vec{J}_2\vec{J}_3 + \mathcal{A}_{(J)}\hat{J}^2,\end{aligned}$$

where $\hat{H}'_2$ is obtained from $\hat{H}_2$ by subtracting the rotational term $A_2\hat{J}^2_2$.

The formalism described above is called the extended CSM (ECSM).

C. Extension to the $K^\pi = 1^\pm$ bands.

Here, the ECSM will be further extended by considering the dipole parity partner bands [12, 13]. The difficulty encountered when the restricted collective space is enlarged consists in finding an intrinsic state which is orthogonal on the previously defined model states, before as well as after angular momentum projection. The second step is to correct the model Hamiltonian by a term so that the resulting Hamiltonian is effective in the extended space of projected states. A possible solution for the intrinsic state generating the dipole bands is:

$$\Psi^{(1,\pm)} = \Omega^\dagger_3 b^\dagger_{31}\Psi^{(\pm)}_g,\ \Omega^\dagger_3 = [b^\dagger_3 b^\dagger_3]_0 + \frac{f^2}{\sqrt{7}}. \tag{2.16}$$

From these states, two sets of angular momentum projected states are obtained, which are hereafter denoted by $\phi^{1,\pm}_{JM}$. These states are weakly coupled to the states of other bands by the $\mathcal{B}_1$ and $\mathcal{B}_3$ terms. Moreover, these terms give large contribution to the diagonal matrix elements involving the projected dipole states. Aiming at describing quantitatively the properties of the dipole states, two terms are added to the model Hamiltonian

$$\Delta H = \mathcal{C}_1\Omega^\dagger_3\Omega_3 + \mathcal{C}_2\Omega^\dagger_3\hat{N}_2\Omega_3. \tag{2.17}$$

The new terms affect only the diagonal m.e. of the dipole states. $\mathcal{C}_2$ is determined so that the corresponding contribution to a particular state (say 2^-) cancels the one coming from the $\mathcal{B}_1$ term. $\mathcal{C}_1$ is determined so that the measured excitation energy of the state 1^- is reproduced. The contribution of the $\mathcal{B}_1$ and $\mathcal{B}_3$ terms to the off-diagonal matrix elements characterizing the dipole states amounts to few keV.

Thus, the final Hamiltonian to be used for describing simultaneously four positive and four negative bands, is:

$$\begin{aligned} H &= \mathcal{A}_1(22\hat{N}_2 + 5\Omega^\dagger_{\beta'}\Omega_{\beta'}) + \mathcal{A}_2\Omega^\dagger_\beta\Omega_\beta + \mathcal{A}_J\vec{J}^2 \\ &+ \mathcal{B}_3\hat{N}_3 + \mathcal{B}_1\hat{N}_3(22\hat{N}_2 + 5\Omega^\dagger_{\beta'}\Omega_{\beta'}) + \mathcal{A}_{(J23)}\vec{J}_2\vec{J}_3 \\ &+ \mathcal{C}_1\Omega^\dagger_3\Omega_3 + \mathcal{C}_2\Omega^\dagger_3\hat{N}_2\Omega_3. \end{aligned} \tag{2.18}$$

The quantities which are to be calculated are:

- The excitation energies

$$\epsilon^{(k)}_J = E^{(k)}_J - E^{(+)}_0 \ . \tag{2.19}$$

- The dynamic moment of inertia, as function of angular frequency.

$$\begin{aligned} \hbar\omega &= \frac{dE}{dI} \approx \frac{1}{2}(E_I - E_{I-2}), \\ \mathcal{J}^{(2)}/\hbar^2 &= \left(\frac{d\omega}{dI}\right)^{-1} \approx 2/(\omega_I - \omega_{I-2}). \end{aligned} \tag{2.20}$$

- The energy displacement functions

$$\begin{aligned} \delta E(J^-) &= E(J^-) \\ &- \frac{(J+1)E((J-1)^+) + JE((J+1)^+)}{2J+1}, \end{aligned} \tag{2.21}$$

$$\begin{aligned} \Delta E_{1,\gamma}(I) &= \frac{1}{16}[6E_{1,\gamma}(I) - 4E_{1,\gamma}(I-1) - 4E_{1,\gamma}(I+1) \\ &+ E_{1,\gamma}(I-2) + E_{1,\gamma}(I+2)], \end{aligned} \tag{2.22}$$

$$E_{1,\gamma}(I) = E(I+1) - E(I).$$

- The E1 transition operator is defined as:

$$\begin{aligned} T_{1\mu} = q_1 \sum_{\mu_2,\mu_3} C^{3\ \ 2\ \ 1}_{\mu_3\ \mu_2\ \mu} \quad & (b^+_{3\mu_3} + (-)^{\mu_3} b_{3,-\mu_3}) \\ & \times\ (b^+_{2\mu_2} + (-)^{\mu_2} b_{2,-\mu_2}) \end{aligned}$$

- Using this transition operator we calculated the ratio:

$$R_1(I) = \frac{B(E1; I^- \to (I+1)^+)}{B(E1; I^- \to (I-1)^+)} \tag{2.23}$$

- Also, the E2 and E3 transition probabilities have been calculated:

$$T_{\lambda\mu} = q_\lambda \left(b^\dagger_{\lambda\mu} + (-)^\mu b_{\lambda,-\mu}\right), \lambda = 2, 3. \tag{2.24}$$

- The angle between the angular momenta $\vec{J}_2$ and $\vec{J}_3$.

$$cos\varphi = \frac{\langle\phi^{(k)}_{JM}|\vec{J}_2.\vec{J}_3|\phi^{(k)}_{JM}\rangle}{\sqrt{\langle\phi^{(k)}_{JM}|\hat{J}^2_2|\phi^{(k)}_{JM}\rangle\langle\phi^{(k)}_{JM}|\hat{J}^2_3|\phi^{(k)}_{JM}\rangle}}, k = 1, \pm. \tag{2.25}$$

D. Numerical results

Numerical calculations have been performed for: ^{158}Ga, ^{172}Yb, ^{218}Ra, ^{220}Ra, ^{226}Ra, ^{228}Th, ^{232}Th, ^{236}U, ^{238}U, ^{238}Pu. Due to the lack of space we do not present here all results, but only those which are necessary for underlying the relevant ideas. There are several parameters involved in the game, which are to be determined through a fitting procedure: $\mathcal{A}_1, \mathcal{A}_2, \mathcal{A}_J, \mathcal{B}_1, \mathcal{B}_3, \mathcal{A}_{(J23)}, \mathcal{C}_1, \mathcal{C}_2, d, f$.

The structure coefficients $\mathcal{A}$ and $\mathcal{B}$ and the deformation parameters d and f were determined by the least square procedure of the excitation energies in the bands $g^{\pm}, \beta^{\pm}, \gamma^{\pm}$. The remaining two parameters $\mathcal{C}_1$ and $\mathcal{C}_2$ are determined as explained before.

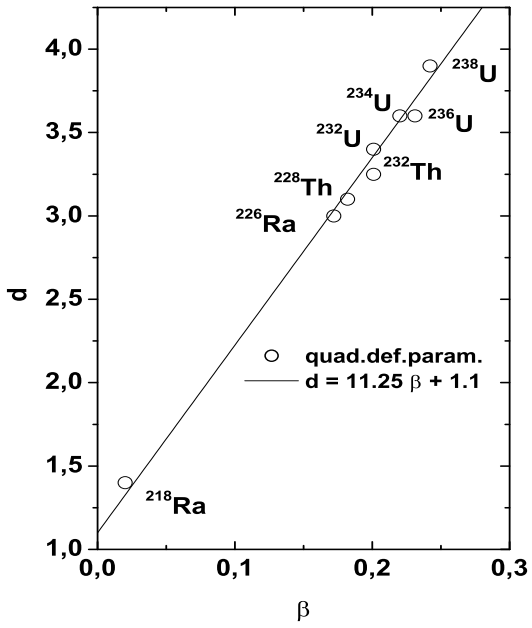

FIG. 1: The deformation parameter d, is plotted as function of the nuclear deformation.

In Fig. 1 the obtained values for the deformation parameter d are plotted as function of the nuclear deformation β, for the actinide isotopes considered. The results for the rare earth isotopes lye on a straight line parallel to the one from Fig . 1. The values of d corresponding to ^{158}Gd and ^{172}Yb are equal to 3 and 3.68, respectively. It is remarkable the linear dependence of the two variables, d and β. Unfortunately, a similar plot for the octupole deformation parameter is not possible due to the lack of experimental data for the nuclear octupole deformation. The calculated

values of f are equal to 0.3 except those for ^{226}Ra and ^{238}U which are 0.8 and 0.6, respectively.

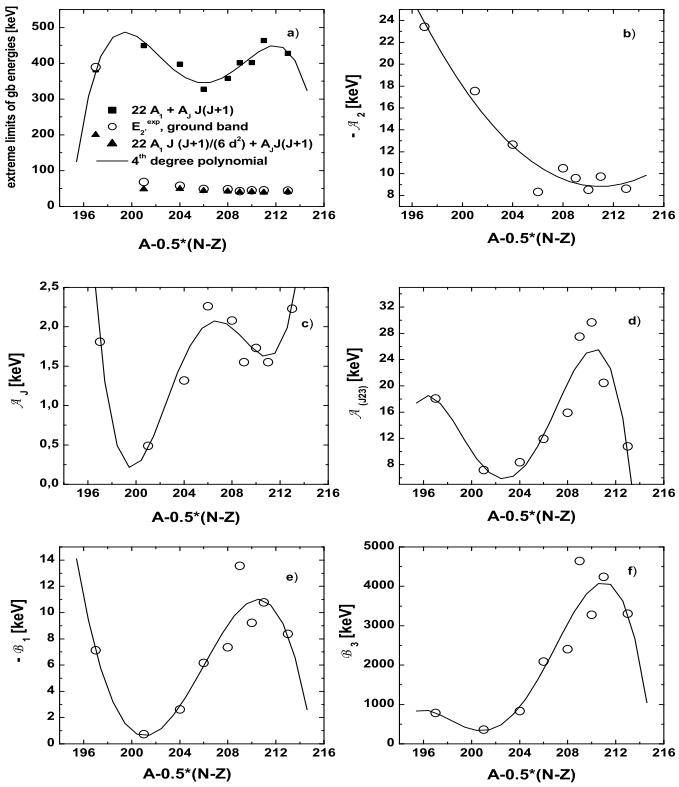

FIG. 2: The coefficients involved in the model Hamiltonian are plotted as function of $A-0.5*(N-Z)$

.

The structure coefficients are represented as function of $A - 0.5(N - Z)$ in Figs. 2 and 3. The calculated values were interpolated by a smooth curve of a polynomial type. Energies for the partner bands g^+ and g^-, in three isotopes of Ra are represented in Fig. 4. One notes the doublet as well as the interleaved structure of positive and negative parity states. In the formalism described here, the doublets are caused by the small octupole deformation. If the octupole deformation were vanishing, the doublet members would be degenerate. For ^{218}Ra the doublet structure persists also in the region of high spin, while for ^{226}Ra the spectrum in the high angular momentum area becomes equidistant.

Let us now turn our attention to the low position of the $K^\pi = 0^-$ state 1^-. This is caused by the term $\vec{J}_2\vec{J}_3$ which is attractive in the state 1^- and repulsive in other states.

The calculated energies for three pairs of parity partner bands, $g^\pm$, $\beta^\pm$ and $\gamma^\pm$, are compared with the available experimental data in Fig.5. There we give also the parabola $aJ(J + 1) + b$

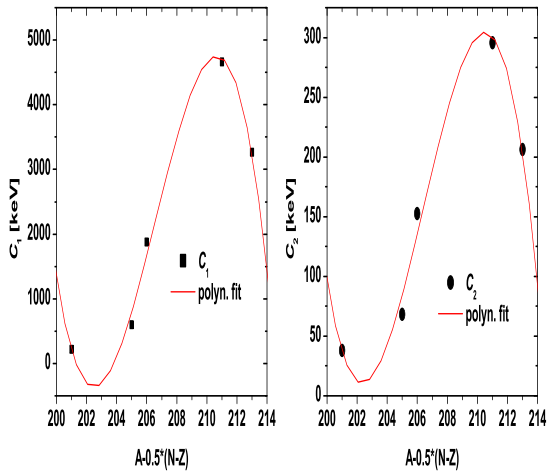

FIG. 3: The structure coefficient $\mathcal{C}_1$ (black square) and $\mathcal{C}_2$, determined as explained in the text, is represented as function of $A - 0.5 * (N - Z)$ (black square). The obtained values are interpolated by a third order polynomial (full line curve).

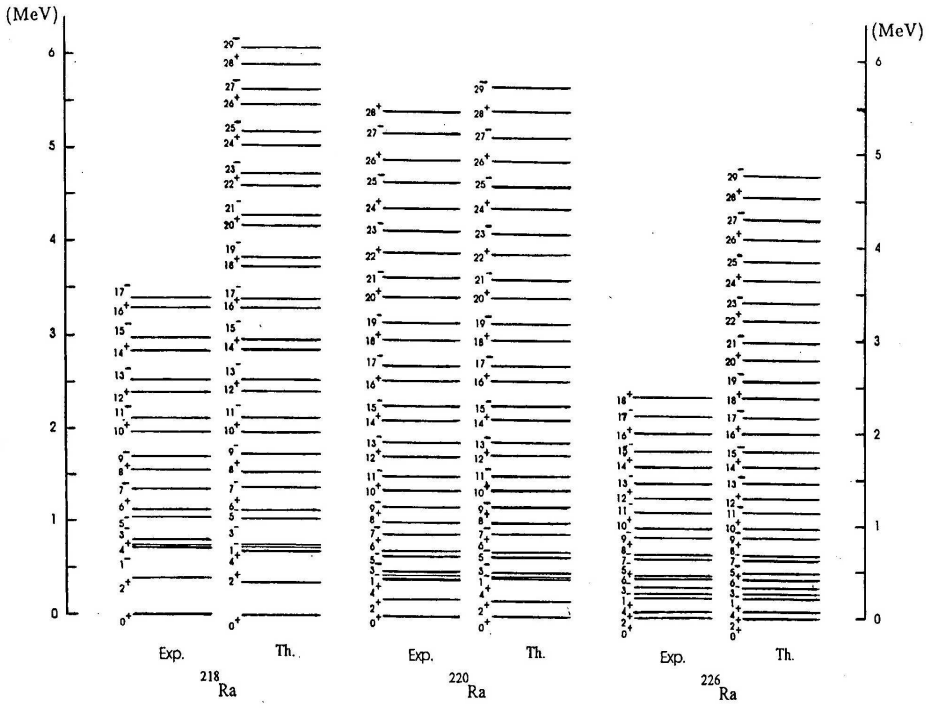

FIG. 4: Experimental and calculated energies for the $g^{\pm}$ bands in ^{218,220,226}Ra (see Ref.[7]).

which fits the energies of the first and the last states in the respective band. In general, the J

dependence of energies is different from the J(J+1) pattern. The quality of the agreement between the theoretical results and the experimental energies can be best judged by plotting the dynamic moment of inertia which is a very sensitive function of the rotational frequency. Such a plot is shown in Fig. 6 for the pairs of bands $g^{\pm}, \beta^{\pm}, \gamma^{\pm}$. This graph indicates ^{226}Ra as the best candidate for a static octupole deformation in all three bands.

Since in ^{218}Ra the spectrum in the bands $g^{\pm}$ is almost equidistant, the dynamic moment of inertia is very large. Due to this feature, for this case we give, instead, the graph, Fig. 7, representing the angular momentum as function of the rotational frequency. It is worth noticing that the back and forward bending seen for the experimental energies characterizing the band g^{+}, are nicely reproduced by our calculations. The microscopic interpretation of the first bending is the crossing of a collective band with a two quasiparticle band, while the forward bending is caused by the intersection of the later band with a four quasiparticle band. In our phenomenological description the two bending are caused by the interaction between the quadrupole and octupole degrees of freedom. If the octupole deformation is small the projected states J^{+}, $(J+1)^{-}$ are close

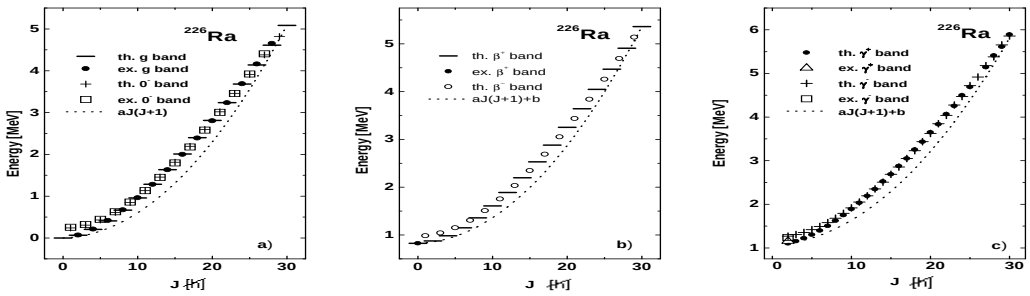

FIG. 5: Experimental and calculated energies for the bands $g^{\pm}, \beta^{\pm}, \gamma^{\pm}$ for ^{226}Ra.

in energies. Since the projected states originates from the same intrinsic state, they are characterized by a single moment of inertia. If the state energies depend linearly on $J(J+1)$ then the first order energy displacement function vanishes for the angular momentum equal to J. If energies depend quadratically on $J(J+1)$, the vanishing of the second order energy displacement function indicates that the second order derivative for energy with respect to $J(J+1)$ is the same for parity partner bands. In order to decide whether a state exhibits a static octupole deformation or not, a simultaneous analysis of both displacement functions is necessary.

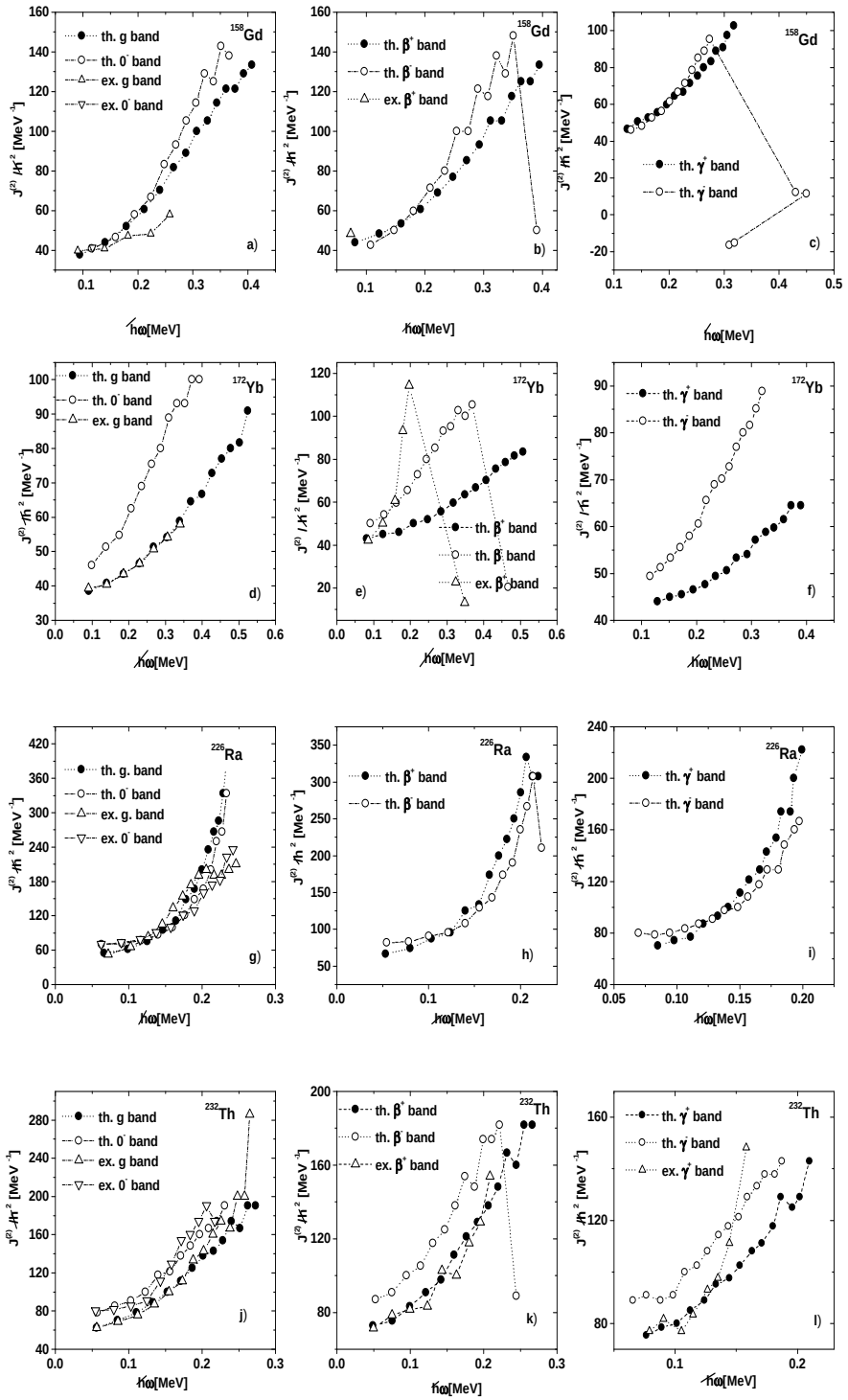

FIG. 6: The dynamic moment of inertia characterizing the bands $g^{\pm}, \beta^{\pm}, \gamma^{\pm}$, is plotted as function of the rotational frequency.

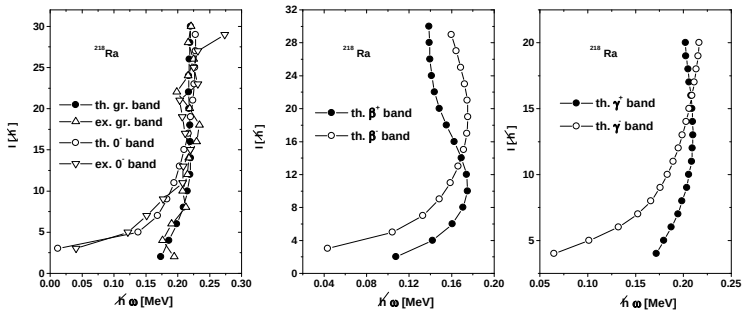

FIG. 7: The angular momentum is plotted as function of the rotational frequency for three parity partner bands, $g^{\pm}, \beta^{\pm}, \gamma^{\pm}$, in ^{218}Ra.

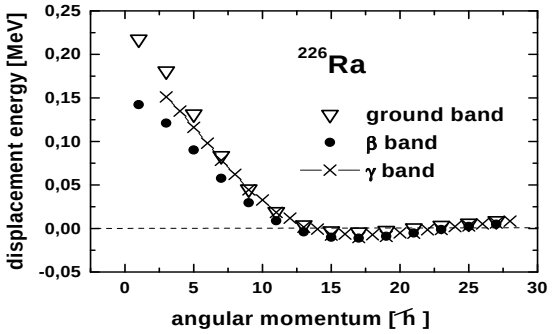

FIG. 8: The first order energy displacement function for ^{226}Ra .

The two functions are given for ^{226}Ra in Figs. 8 and 9, respectively. We note that at least for this isotope the octupole deformation is settled, according to the behavior of the δE function, simultaneously in the three pairs of bands, $g^{\pm}, \beta^{\pm}, \gamma^{\pm}$. The second order energy displacement shows that ground and beta bands get octupole deformation for the same angular momentum while in the gamma bands the octupole deformation is earlier settled. A systematic analysis of the displacement functions for a large number of nuclei may be found in Refs. [10, 22]. Therein we identified several distinct situations: a) octupole deformation shows up in all three pairs of bands; b) octupole deformation appears in the bands $g^{\pm}$ but not in the other bands; c) octupole

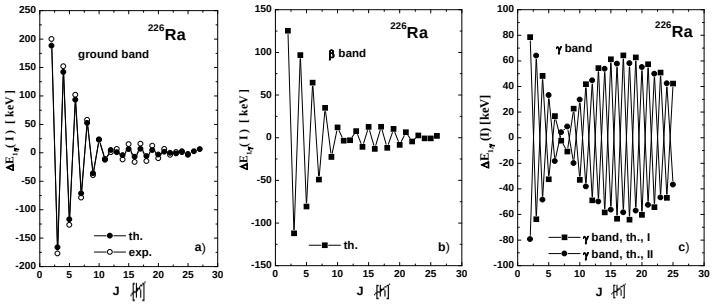

FIG. 9: The second order energy displacement function for ^{226}Ra .

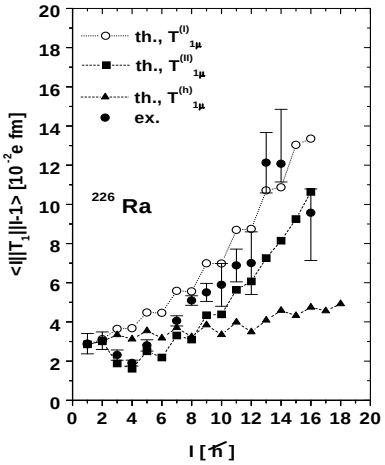

FIG. 10: The matrix elements for the transition $I \rightarrow (I-1)$ is plotted as function of the angular momentum for ^{226}Ra. Data are from Ref. [24]. Calculations correspond to three different expressions for the transition operator as explained in Ref.[11] .

deformation is settled in the $\gamma^{\pm}$ bands but not in the others.

Due to the rod effect saying that the charge density is maximum in the region where the surface curvature is maximum, a system having octupole deformation may exhibit a non-vanishing dipole moment. Consequently, interacting with an electromagnetic field such a system can be driven in a state characterized by large E1 rates. In this context one expects that the B(E1) value exhibits a jump at the angular momentum where the octupole deformation is set on. This feature is illustrated

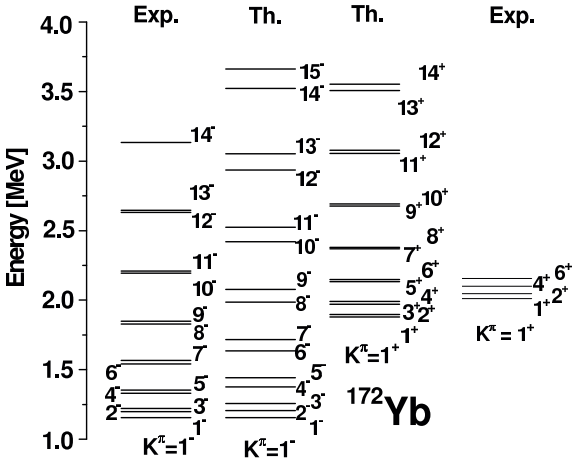

FIG. 11: Theoretical (Th.) and available experimental (Exp.) excitation energies for the $K^\pi = 1^-$ and $K^\pi = 1^+$ in ^{172}Yb.

in Fig.10 where the reduced matrix element for the transition $I \to (I-1)$ is represented as function of angular momentum. One notes a fairly good agreement between theoretical and experimental data.

The results for the $K^\pi = 1^-$ band energies are presented in Fig.11 for ^{172}Yb, where relevant data are available [23]. In Fig. 12 the dynamic moment of inertia is plotted vs. the angular momentum. From this figure one notices that the results corresponding to even and those corresponding to odd angular momenta are lying on separate smooth curves as if these sets of states belonged to two distinct bands. The remark is valid for both the positive and negative parity bands.

In order to see whether there are signatures of octupole deformation in the dipole bands, we show in Fig. 13 the energy displacement functions for the two dipole bands with $K^\pi = 1^\pm$.

According to Fig.13 , the states of angular momentum equal to 18,19 may have static octupole deformation. To obtain a definite conclusion about the static octupole deformation we have analyzed the E1 and M1 properties of these bands. The relative magnitude of branching ratios for the bands with $K^\pi = 1^+$ and $K^\pi = 1^-$ indicate that the magnetic transitions are stronger for the positive parity states while the E1 transitions prevail for negative parity states. Due to this fact we call the band $K^\pi = 1^+$ as *the magnetic band* while the negative parity band as *the electric band*. The branching ratios of the dipole states calculated within the formalism presented above are compared with the corresponding data in Fig.14. In contrast to the case of $K^\pi = 0^-$ band, for the $K^\pi = 1^-$ band there is no jump in the behavior of the B(E1) value. However, the M1 branching ratio from the $K^\pi = 1^+$ to $K^\pi = 0^+$ get a jump for $J = 18, 19$, which are in fact the angular

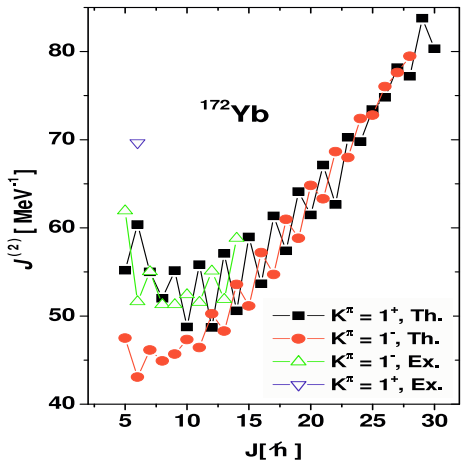

FIG. 12: The dynamic moment of inertia for the dipole bands of positive and negative parity corresponding to the calculated and experimental energies respectively, is plotted as function of the angular momentum

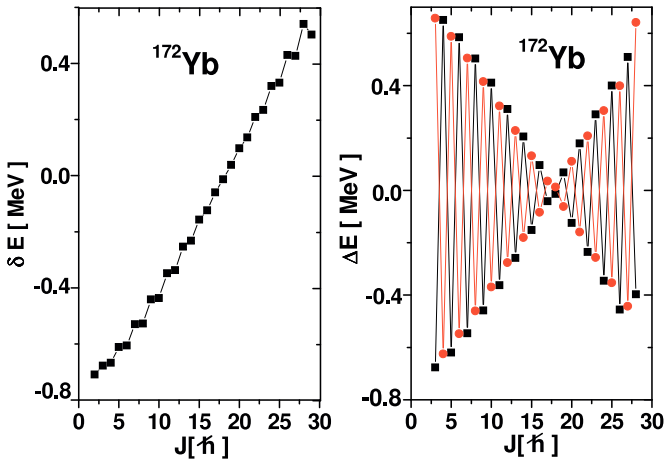

FIG. 13: The energy displacement functions δE (left panel) and ΔE (right panel), given in the text, are plotted as functions of J.

momenta where the energy displacement functions vanish. Due to this feature we consider the big value of the mentioned M1 branching ratio as a signature for the octupole deformation in the dipole bands. Within ECSM, one can calculate the angle between the angular momenta carried by the quadrupole ($\vec{J}_2$) and octupole ($\vec{J}_3$) bosons respectively, for a state of total angular momentum $\vec{J}$. This angle is shown in Fig. 15 as function of the angular momentum for the states belonging to the four pairs of bands under study. Apart from small details, the features shown in Fig. 15 for

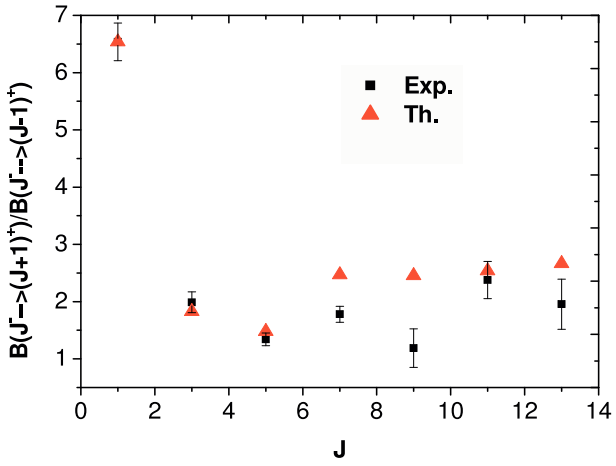

FIG. 14: The branching ratios characterizing the transitions of $K^\pi = 1^-$ states to the ground band states (triangle), are compared with the corresponding experimental data (square). The transition operator used is $T_{1\mu} = T^h_{1\mu} + T^{anh}_{1\mu}$ with the harmonic term defined in the text and $T^{anh}_{1\mu} = q_{anh}\{\left[b^\dagger_3 \left(\hat{J}_3\hat{J}_2\right)_2\right]_{1\mu} + \left[\left(\hat{J}_3\hat{J}_2\right)_2 b_{\tilde{3}}\right]_{1\mu}\}$. All ratios correspond to the relative effective charge q_{anh}/q_1=-1.722, where q_1 denotes the strength of the harmonic term.

^{226}Ra are common to all nuclei studied by our group. The angle has a saw-tooth structure for the dipole bands. Here the angle characterizing the even and odd angular momenta stay on separate smooth curves suggesting once again that the two sets of states might form different bands. For the bands $g^\pm, \beta^\pm, \gamma^\pm$ the angle is decreasing up to a critical value after which is slightly increasing reaching a plateau at $\varphi = \pi/2$. The interpretation of this result is as follows. If the quadrupole bosons describes an ellipsoidal shape having the axis OZ as symmetry axis, the angular momentum $\vec{J}_2$ is oriented along an axis in the plane XOY, say OX, to which the maximum moment of inertia is associated. The octupole bosons describe a shape for which the moment of inertia corresponding to the axis OZ, is maximum.

Suppose now that a term describing a set of particles and a term describing the interaction between the two sub-systems are added to the model Hamiltonian. Depending on the strength of the interaction, the eigenstates of the resulting Hamiltonian may be characterized by a right or left triad $(\vec{j}, \vec{J}_2, \vec{J}_3)$. In the case the two frames defines states of equal energies one says that the composite system exhibits a chiral symmetry. In this context we may say that the nuclear system excited in a high angular momentum state belonging to either of the six bands $g^\pm, \beta^\pm, \gamma^\pm$, constitutes a precursor of a chiral symmetry system. Such a system will be studied in Section 3.

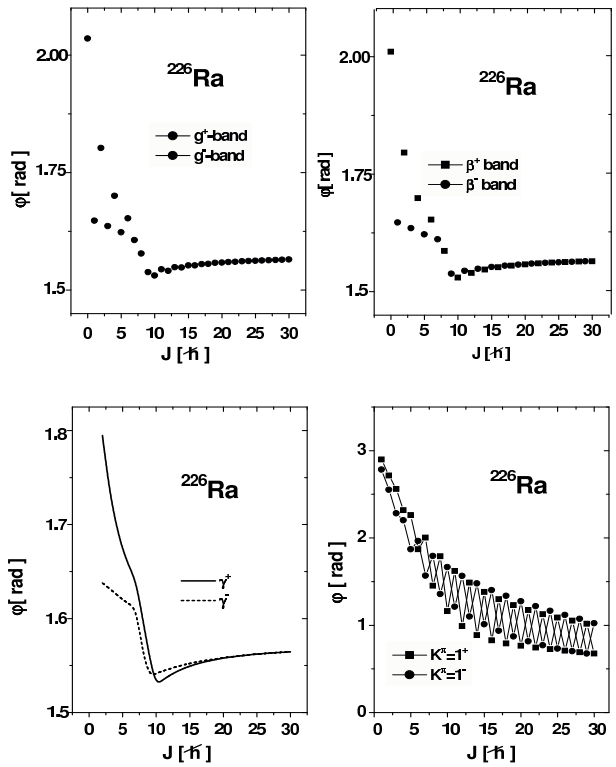

FIG. 15: The angle between the angular momenta carried by the quadrupole and octupole bosons respectively, in the states of $g^{\pm}$ (upper left), $\beta^{\pm}$ (upper right), $\gamma^{\pm}$ (bottom left) and dipole (bottom right) bands, vs. angular momentum.

We may ask ourself whether the magnetic states described in this lecture is related with the scissors mode [25]. The scissors mode describes the angular oscillations of the symmetry axes of proton and neutron systems. Here, we do not make any distinction between protons and neutrons, but we could say that we deal with two distinct entities, one described by the quadrupole and other by octupole bosons. The two systems rotate around axes which make an angle which was just described. By contrast to the scissors mode, where the angle between the symmetry axes is small, here the angle is large. Therefore, we could name the magnetic states described in the present lecture as shares states.

III. ROTATIONAL BANDS IN EVEN-ODD NUCLEI

A. The model Hamiltonian

We suppose that the rotational bands in even-odd nuclei may be described by a particle-core Hamiltonian:

$$H = H_{sp} + H_{core} + H_{pc}, \tag{3.1}$$

where H_{sp} is a spherical shell model Hamiltonian associated to the odd nucleon, while H_{core} is a phenomenological Hamiltonian which describes the collective motion of the core in terms of quadrupole and octupole bosons. This term is identical to that used[**?**] in the previous Section to describe eight rotational bands in even-even nuclei. The two subsystems interact with each other by H_{pc}, which has the following expression:

$$\begin{aligned} H_{pc} = & - X_2 \sum_{\mu} r^2 Y_{2,-\mu}(-)^{\mu} \left(b^{\dagger}_{2\mu} + (-)^{\mu} b_{2,-\mu} \right) - X_3 \sum_{\mu} r^3 Y_{3,-\mu}(-)^{\mu} \left(b^{\dagger}_{3\mu} + (-)^{\mu} b_{3,-\mu} \right) \\ & + X_{jJ} \vec{j}\vec{J} + X_{I^2} \vec{I}^2. \end{aligned} \tag{3.2}$$

The term $\vec{j}\vec{J}$ is similar to the spin-orbit interaction from the shell model and expresses the interaction between the angular momenta of the odd-particle and the core. The last term is due to the rotational motion of the whole system, $\vec{I}$ denoting the total angular momentum of the particle-core system. The core states are described by eight sets of mutually orthogonal functions, obtained by projecting out the angular momentum and the parity from four quadrupole and octupole deformed functions: one is a product of two coherent states:

$$\Psi_g = e^{f(b^{+}_{30} - b_{30})} e^{d(b^{+}_{20} - b_{20})} |0\rangle_2 |0\rangle_3 \equiv \Psi_o \Psi_q |0\rangle_2 |0\rangle_3, \tag{3.3}$$

while the remaining three are polynomial boson excitations of Ψ_g. The parameters d and f are real numbers and simulate the quadrupole and octupole deformations, respectively. The vacuum state for the k-pole boson, $k = 2, 3$, is denoted by $|0\rangle_k$.

The particle-core interaction generates a deformation for the single particle trajectories. Indeed, averaging the model Hamiltonian with Ψ_g, one obtains a deformed single particle Hamiltonian, H_{mf} which plays the role of the mean field for the particle motion:

$$H_{mf} = \mathcal{C} + H_{sp} - 2dX_2 r^2 Y_{20} - 2fX_3 r^3 Y_{30}, \tag{3.4}$$

where $\mathcal{C}$ is a constant determined by the average of H_{core}. The Hamiltonian H_{mf} represents an extension of the Nilsson Hamiltonian by adding the octupole deformation term. In Ref.[18] we

have shown that in order to get the right deformation dependence of the single particle energies H_{mf} must be amended with a monopole-monopole interaction, $M\omega^2 r^2 \alpha_{00} Y_{00}$, where the monopole coordinate α_{00} is to be determined from the volume conservation restriction. This term has a constant contribution within a band. The constant value is, however, band dependent.

In order to find the eigenvalues of the model Hamiltonian we follow several steps:

1) In principle the single particle basis could be determined by diagonalizing H_{mf} amended with the monopole interaction. The product basis for particle and core may be further used to find the eigenvalues of H. Due to some technical difficulties in restoring the rotation and space reversal symmetries for the composite system wave function, this procedure is however tedious and therefore we prefer a simpler method. Thus, the single particle space consists of three spherical shell model states with angular momenta j_1, j_2, j_3. We suppose that j_1 and j_2 have the parity $\pi = +$, while j_3 has a negative parity $\pi = -$. Due to the quadrupole-quadrupole interaction the odd particle from the state j_1 can be promoted to j_2 and vice-versa. The octupole-octupole interaction connects the states j_1 and j_2 with j_3. Due to the above mentioned effects the spherical and space reversal symmetries of the single particle motion are broken. To be more specific, by diagonalizing H (3.1) in a projected spherical particle-core basis with the spherical single particle state factors mentioned above, the eigenstates could be written as a projected spherical particle-core state having as single particle state factor a function without rotation and parity good symmetries. Therefore one could start with a coupled basis where the single particle state is a linear combination of the spherical states, where the mixing coefficients are to be determined by a least square fitting procedure as to obtain an optimal description of the experimental excitation energies. Thus, instead of dealing with a spherical shell model state coupled to a deformed core without reflection symmetry, as the traditional particle-core approaches proceed, here the single particle orbits are lacking the spherical and space reversal symmetries and by this, their symmetry properties are consistent with those of the phenomenological core.

2) We remark that Ψ_g is a sum of two states of different parities. This happens due to the specific structure of the octupole coherent state:

$$\Psi_o = \Psi_o^{(+)} + \Psi_o^{(-)}. \tag{3.5}$$

The states of a given angular momentum and positive parity can be obtained through projection

from the intrinsic states:

$$|n_1 l_1 j_1 K\rangle \Psi_o^{(+)} \Psi_q, \;\; |n_2 l_2 j_2 K\rangle \Psi_o^{(+)} \Psi_q, \;\; |n_3 l_3 j_3 K\rangle \Psi_o^{(-)} \Psi_q. \tag{3.6}$$

The projected states of negative parity are obtained from the states:

$$|n_1 l_1 j_1 K\rangle \Psi_o^{(-)} \Psi_q, \;\; |n_2 l_2 j_2 K\rangle \Psi_o^{(-)} \Psi_q, \;\; |n_3 l_3 j_3 K\rangle \Psi_o^{(+)} \Psi_q. \tag{3.7}$$

The angular momentum and parity projected states are denoted by:

$$\begin{aligned}
\varphi^{(+)}_{IM}(j_i K; d, f) &= N^{(+)}_{i;IK} P^I_{MK} |n_i l_i j_i K\rangle \Psi_o^{(+)} \Psi_q \equiv N^{(+)}_{i;IK} \psi^{(+)}_{IM}(j_i K; d, f), i = 1, 2 \\
\varphi^{(+)}_{IM}(j_3 K; d, f) &= N^{(+)}_{3;IK} P^I_{MK} |n_3 l_3 j_3 K\rangle \Psi_o^{(-)} \Psi_q \equiv N^{(+)}_{3;IK} \psi^{(+)}_{IM}(j_3 K; d, f), \\
\varphi^{(-)}_{IM}(j_i K; d, f) &= N^{(-)}_{i;IK} P^I_{MK} |n_i l_i j_i K\rangle \Psi_o^{(-)} \Psi_q \equiv N^{(-)}_{i;IK} \psi^{(-)}_{IM}(j_i K; d, f), i = 1, 2 \\
\varphi^{(-)}_{IM}(j_3 K; d, f) &= N^{(-)}_{3;IK} P^I_{MK} |n_3 l_3 j_3 K\rangle \Psi_o^{(+)} \Psi_q \equiv N^{(-)}_{3;IK} \psi^{(-)}_{IM}(j_3 K; d, f).
\end{aligned} \tag{3.8}$$

The factors $N^{(\pm)}_{i,IK}$ asure that the projected states $\varphi^{(\pm)}$ are normalized to unity. Obviously, the unnormalized projected states are denoted by $\psi^{(\pm)}$. For the quantum number K we consider the lowest three values, i.e. $K = 1/2, 3/2, 5/2$. Note that the earlier particle-core approaches [27, 28] restrict the single particle space to a single j, which results in eliminating the contribution of the octupole-octupole interaction.

3) Note that for a given j_i, the projected states with different K are not orthogonal. Indeed, the overlap matrices :

$$\begin{aligned}
A^{(+)}_{K,K'}(I j_l; d, f) &= \langle \psi^{(+)}_{IM}(j_l K; d, f) | \psi^{(+)}_{IM}(j_l K'; d, f) \rangle, \\
l &= 1, 2, 3; \;\; K, K' = 1/2, 3/2, 5/2, \\
A^{(-)}_{K,K'}(I j_l; d, f) &= \langle \psi^{(-)}_{IM}(j_l K; d, f) | \psi^{(-)}_{IM}(j_l K'; d, f) \rangle, \\
l &= 1, 2, 3; \;\; K, K' = 1/2, 3/2, 5/2,
\end{aligned} \tag{3.9}$$

are not diagonal. By diagonalization, one obtains the eigenvalues $a^{(\pm)}_{Ip}(j_l)$ and the corresponding eigenvectors $V^{(\pm)}_{IK}(j_l, p)$, with $K = 1/2, 3/2, 5/2$ and $p = 1, 2, 3$. Then, the functions:

$$\begin{aligned}
\Psi^{(+)}_{IM}(j_l, p; d, f) &= N^{(+)}_{l;Ip} \sum_K V^{(+)}_{IK}(j_l, p) \psi^{(+)}_{IM}(j_l K; d, f), \\
\Psi^{(-)}_{IM}(j_l, p; d, f) &= N^{(-)}_{l;Ip} \sum_K V^{(-)}_{IK}(j_l, p) \psi^{(-)}_{IM}(j_l K; d, f).
\end{aligned} \tag{3.10}$$

are mutually orthogonal. The norms are given by:

$$\left(N_{l;Ip}^{(\pm)}\right)^{-1} = \sqrt{a_{Ip}^{(\pm)}(j_l)}. \tag{3.11}$$

For each state, there is a term in the sum (3.10), which has a maximal weight. The corresponding quantum number K is conventionally assigned to the mixed state. 4) In order to simulate the core deformation effect on the single particle motion, in some cases the projected states corresponding to different j must be mixed up.

$$\begin{aligned}
\Phi_{IM}^{(+)}(p;d,f) &= \sum_{l=1,2,3} \mathcal{A}_{pl}^{(+)} \Psi_{IM}^{(+)}(j_l p;d,f), \\
\Phi_{IM}^{(-)}(p;d,f) &= \sum_{l=1,2,3} \mathcal{A}_{pl}^{(-)} \Psi_{IM}^{(-)}(j_l p;d,f).
\end{aligned} \tag{3.12}$$

The amplitudes $\mathcal{A}_{pl}^{(\pm)}$ can be obtained either by diagonalizing H_{mf} or, as we mentioned before, by a least square fitting procedure applied to the excitation energies.

The energies of the odd system are approximated by the average values of the model Hamiltonian corresponding to the projected states:

$$\begin{aligned}
E_I^{(+)}(p;d,f) &= \langle \Phi_{IM}^{(+)}(p;d,f)|H|\Phi_{IM}^{(+)}(p;d,f)\rangle, \\
E_I^{(-)}(p;d,f) &= \langle \Phi_{IM}^{(-)}(p;d,f)|H|\Phi_{IM}^{(-)}(p;d,f)\rangle.
\end{aligned} \tag{3.13}$$

Note that due to the structure of the particle-core projected states, the energis for the odd system are determined by the coupling of the odd particle to the excited states of the core. Our approach was applied for the description of the $K^\pi = 1/2^\pm$ bands.

However this procedure can be extended by including the $K \neq 0$ states in the space describing the deformed core.

B. The description of the $K^\pi = \frac{3}{2}^\pm, \frac{5}{2}^\pm$ bands.

In principle the method presented in the previous subsection may work for the description of bands with the quantum number larger than 1/2. However the intrinsic reference frame for the odd system is determined by the deformed core and therefore one expects that this brings an important contribution to the quantum number K. To be more specific, we cannot expect that projecting out the good angular momentum from $|j5/2\rangle \otimes \Psi_g$ a realistic description of the $K = 5/2$ bands is

obtained. Therefore we assume that the $K^\pi = \frac{3}{2}^\pm, \frac{5}{2}^\pm$ bands are described by projecting out the angular momentum from a product state of a low K single partile state and the intrinsic gamma band state.

We recall that within CSM, the states of the gamma band are obtained by projection from the intrinsic state:

$$\Psi_2^{(\gamma;\pm)} = \Omega^\dagger_{\gamma,2}\Psi_o^{(\pm)}\Psi_q \tag{3.14}$$

where the excitation operator for the gamma intrinsic state was defined before. The low index of Ψ in Eq. (3.14) is the K quantum number for the γ intrinsic state. Thus, a simultaneous description of the bands with $K = 1/2, 3/2, 5/2$ can be achieved with the projected states:

$$\begin{aligned}
\varphi^{(\pm)}_{IM;1/2} &= N^{(\pm)}_{I,1/2}\sum_J \left(N^{(g,\pm)}_J\right)^{-1} C^{j_1\ J\ I}_{1/2\ 0\ 1/2}\left[|n_1l_1j_1\rangle \otimes \varphi^{(g;\pm)}_J\right]_{IM},\\
\varphi^{(\pm)}_{IM;3/2} &= N^{(\pm)}_{I,3/2}\sum_J \left(N^{(\gamma,\pm)}_J\right)^{-1} C^{j_1\ J\ I}_{-1/2\ 2\ 3/2}\left[|n_2l_2j_2\rangle \otimes \varphi^{(\gamma;\pm)}_J\right]_{IM},\\
\varphi^{(\pm)}_{IM;5/2} &= N^{(\pm)}_{I,5/2}\sum_J \left(N^{(\gamma,\pm)}_J\right)^{-1} C^{j_1\ J\ I}_{1/2\ 2\ 5/2}\left[|n_3l_3j_3\rangle \otimes \varphi^{(\pm)}_J\right]_{IM}.
\end{aligned} \tag{3.15}$$

In the above expressions the notation $N^{(i,\pm)}_J$ with $i = g, \gamma$ is used for the normalization factors of the projected states describing the ground and the gamma bands, respectively, of the even-even core. Note that for each angular momentum I the above set of three projected states is orthogonal. The energies for the six bands with $K^\pi = 1/2^\pm, 3/2^\pm, 5/2^\pm$ are obtained by averaging the model Hamiltonian (3.1) with the projected states defined above.

$$E_{I,K} = \langle\varphi^{(\pm)}_{IM;K}|H|\varphi^{(\pm)}_{IM;K}\rangle, K = 1/2, 3/2, 5/2. \tag{3.16}$$

The matrix elements of the particle core-interaction can be analytically calculated [29].

C. Transition probabilities

For some $K = 1/2$ bands results for the reduced $E1$ and $E2$ transition probabilities are available. They are given in terms of the branching ratios:

$$R_{I^\pi} = \frac{B(E1; I^\pi \to (I-1)^{\pi'})}{B(E2; I^\pi \to (I-2)^\pi)}, \pi' \neq \pi \tag{3.17}$$

The dipole and quadrupole transition operators are:

$$\begin{aligned}
Q_{1\mu} &= eq_1\left((b^\dagger_2 b^\dagger_3)_{1\mu} + (b_3b_2)_{\widetilde{1\mu}}\right),\\
Q_{2\mu} &= eQ_2\left(b^\dagger_{2\mu} + (-)^\mu b_{2,-\mu} + ar^2Y_{2\mu}\right).
\end{aligned} \tag{3.18}$$

D. Numerical results

Excitation energies for one positive and one negative parity bands in three odd isotopes:^{219}Ra, ^{237}U and ^{239}Pu have been calculated. The parameters defining H_{core}, as well as the deformation parameters d and f are the same as for the eight rotational bands in the even-even neighboring isotopes. The single particle states are spherical shell model states with the appropriate parameters for the (N, Z) region of the considered isotopes [30]. Our calculations correspond to the single particle states: $(j_1, j_2, j_3) = (2g_{7/2}, 2g_{9/2}, 1h_{9/2})$. In order to obtain the best agreement between the calculated excitation energies and the corresponding experimental data, in the expansion (3.12) a small admixture of the states $(j_1; j_3)$ and $(j_2; j_3)$ was considered: $|\mathcal{A}^{(+)}_{i,3}|^2$ and $|\mathcal{A}^{(-)}_{i,3}|^2$, are both equal to 0.001 for for ^{219}Ra while for ^{237}U and ^{239}Pu the amplitudes take the common values: $|A^{(+)}_{i,3}|^2 = |A^{(-)}_{1,3}|^2 = 0.04$ The mixing amplitude of the states (j_1, j_2) is negligible small. Energies (3.13) depend on the interaction strengths X_2, X_3, X_{jJ} and X_{I^2}. These were determined by fitting four particular energies in the two bands of different parities, i.e. $K^\pi = \frac{1}{2}^\pm$. The results of the fitting procedure are given in Table I. Inserting these in Eqs. (3.13) the energies in the two bands with $K = 1/2$ are readily obtained.

$$E(I^\pm) = E^{(\pm)}_I(1; d, f) - E^{(+)}_{\frac{1}{2}}(1; d, f). \tag{3.19}$$

The theoretical results for excitation energies, given in Fig. 16 and Table II, agree quite well with the corresponding experimental data. Our results suggest that the dominant K component is $K = 1/2$ while the dominant j component is $g_{9/2}$ The results of r.m.s. values for ^{219}Ra, ^{237}U and ^{239}Pu are 66.24 keV, 48.97 keV and 31.8 keV, respectively. In calculating the $r.m.s.$ value for ^{219}Ra we ignored the data for the states $53/2^\pm$ since the spin asignement is unsure. It is interesting to mention that the spectra of ^{219}Ra has been measured by two groups [37, 38] by the same reaction, ^{208}Pb(^{14}C,3n)^{219}Ra. However they assign for the ground state different angular momenta, $9/2^+$ [37] and $7/2^+$ [38]. In our approach both assignements yield good description of the data. However we made the option for $9/2^+$ since the corresponding results agree better with the experimental data than those obtained with the other option.

The case of ^{227}Ra was treated with the formalism presented in Subsection B. The single particle basis is: $2g_{7/2}, 2g_{9/2}, 2f_{5/2}$. The first state coupled to the coherent state describing the unprojected ground state generates the parity partner bands $K^\pi = 1/2^\pm$. The bands $K^\pi = 3/2^\pm$ are obtained through projection from the product state $2g_{9/2}\Psi^{(\gamma;\pm)}_2$ while the bands $K^\pi = 5/2^\pm$ originate from

Parameters	^{219}Ra	^{227}Ra	^{237}U	^{239}Pu
$X_2 b^2$[keV]	22.714	-1.992	1.080	-2.515
$X_3 b^3$[keV]	-8.823	169.511	2.227	4.937
X_{jJ}[keV]	-0.230	8.553	-5.817	-3.985
X_{I^2}[keV]	3.778	4.390	4.634	5.050

TABLE I: Parameters involved in the particle-core Hamiltonian obtained by fitting four excitation energies. Here b denotes the oscillator length: $b = (\frac{\hbar}{M\omega})^{1/2}$; $\hbar\omega = 41A^{-1/3}$. The usual notations for nucleon mass (M) and atomic number (A) were used

.

the intrinsic state $2f_{5/2}\Psi_2^{(\gamma;\mp)}$. Concerning the bands characterized by $K^\pi = 1/2^\pm$ one could consider also the mixing of components with different K in the manner discussed in Section A. However, our numerical application suggests that such a mixing is not really necessary in order to obtain a realistic description of the available data. The calculated energies in the three bands are compared with the corresponding experimental data in Fig.17.

From Fig. 17 we note that our approach reproduces the experimental energies ordering in the band $K^\pi = 1/2^-$ ordering. The energy split of the states $3/2^-, 1/2^-$ is nicely described although the doublet is shifted down by an amount of about 50 keV. In the band $5/2^+$ there exist an energy level which is tentatively asigned with $11/2^+$. Our calculations suggests that this level could be asigned as $13/2^+$. No experimental data are available for the band $5/2^-$. In Fig. 17 we gave however the results of our calculations for this band. Note that the ordering for the lowest levels is not the natural one. However starting with $13/2^-$ the normal ordering is restored. It is interesting to note that the heading states for the bands $1/2^+$ and $5/2^+$ are almost degenerate. the same it is true for the lowest angular momenta states in their negative parity partner bands.

Now we would like to comment on the parameters yielded by the fitting procedure, for the considered isotopes. Except for ^{237}U, where both quadrupole-quadrupole and octupole-octupole interactions are attractive, the two intercations have different characters for the rest of nuclei. In the first situation the λ (=2,3)-pole moments of the odd nucleon and of the collective core have different signs. In the remaining cases the two moments are of similar sign. We also remark the large strength for the $q_3.Q_3$ interaction in ^{227}Ra which is consistent with the fact the neighbouring even-even isotope exhibits a relatively large octupole deformation. Indeed, according to Refs.

	^{219}Ra				^{237}U				^{239}Pu			
	$\pi = +$		$\pi = -$		$\pi = +$		$\pi = -$		$\pi = +$		$\pi = -$	
J	Exp.	Th.	Exp.	Th.	Exp.	Th.	Exp.	Th.	Exp.	Th.		
1/2					0.0	0.0		398.5	0.0	0.0	469.8	469.8
3/2					11.4	11.4		454.4	7.9	7.9	492.1	477.7
5/2					56.3	74.6		475.5	57.3	62.8	505.6	498.3
7/2					82.9	106.9		550.3	75.7	108.4	556.0	549.8
9/2	0.0	0.0			162.3	191.2		581.3	163.8	183.5	583.0	572.0
11/2	539.0	545.0			204.1	231.8		680.9	193.5	222.0	661.2	655.2
13/2	234.3	235.0	588.0	586.0	317.3	347.7	721.9	318.5	338.1	698.7	685.7	
15/2	837.0	847.6	495.4	496.0	375.1	393.1	846.4	846.4	359.2	386.5	806.4	799.9
17/2	529.1	525.4	921.0	917.4	518.2	544.2	930.0	899.1	519.5	534.9	857.5	839.5
19/2	1229.0	1210.6	733.7	734.3	592.0	592.0	1027.5	1046.6	570.9	592.2	992.5	984.2
21/2	876.6	861.2	1309.0	1318.9	762.8	780.3	1131.0	1113.3	764.7	773.7	1058.1	1033.3
23/2	1622.0	1626.6	1035.6	1038.3	853.0	829.0	1250.7	1281.3	828.0	839.2	1219.4	1208.3
25/2	1271.6	1235.5	1722.0	1790.5	1048.7	1065.8	1376.1	1364.8	1053.1	1054.4	1300.9	1267.2
27/2	2022.0	2090.7	1393.6	1400.6	1155.1	1108.8	1515.7	1550.2	1127.8	1127.8	1487.4	1472.2
29/2	1684.7	1644.4	2137.0	2230.5	1372.2	1378.3	1662.3	1654.0	1381.5	1377.0	1584.9	1541.2
31/2	2444.0	2600.9	1815.6	1814.2	1494.1	1421.6	1821.8	1852.8	1467.8	1458.0	1795.4	1776.0
33/2	2113.4	2086.8	2552.0	2580.8	1729.2	1728.7	1987.7	1981.0	1748.5	1744.2	1908.9	1855.4
35/2			2272.1	2272.7	1868.2	1772.5	2166.5	2188.9	1847.0	1831.3	2143.4	2119.8
37/2	2563.6	2563.6	2987.0	3115.9	2117.2	2117.2	2349.7	2346.1	2152.2	2150.2	2272.0	2209.8
39/2			2750.8	2770.6	2272.2	2161.7	2547.5	2558.3	2263.0	2245.0	2529.4	2503.6
41/2	3029.0	3076.7			2530.1	2544.1	2746.7	2749.4	2590.1	2597.9	2672.0	2604.4
43/2			3255.8	3303.4	2702.5	2589.4	2960.5	2960.5	2714.0	2700.5	2951.4	2927.5
45/2	3505.0	3627.9			2963.8	3009.5	3174.7	3191.3	3060.1	3087.5	3108.0	3039.3
47/2			3776.5	3867.8	3154.5	3055.6	3401.5	3395.3	3198.0	3198.0	3407.0	3395.3
49/2	4009.6	4218.7			3415.8	3513.7	3630.0	3671.7	3559.1	3619.1	3578.0	3514.4
51/2			4328.9	4462.5	3625.5	3560.5	3865.0	3862.4	3713.0	3737.0	3895.0	3895.8
53/2	4540.4	4759.2			3886.8	4057.8	4105.0	4190.9	4087.1	4194.0	4080.0	4029.9
55/2			4913.6	5044.1	4115.0	4104.8	4344.0	4350.0	4256.0	4319.8	4413.0	4436.7

TABLE II: Excitation energies in ^{219}Ra, ^{237}U and ^{239}Pu, for the bands characterized by $K^\pi = \frac{1}{2}^+$ and $K^\pi = \frac{1}{2}^-$ respectively, are given in keV. The results of our calculations (Th.) are compared with the corresponding experimental data (Exp.) taken from Ref.[32, 37, 38].

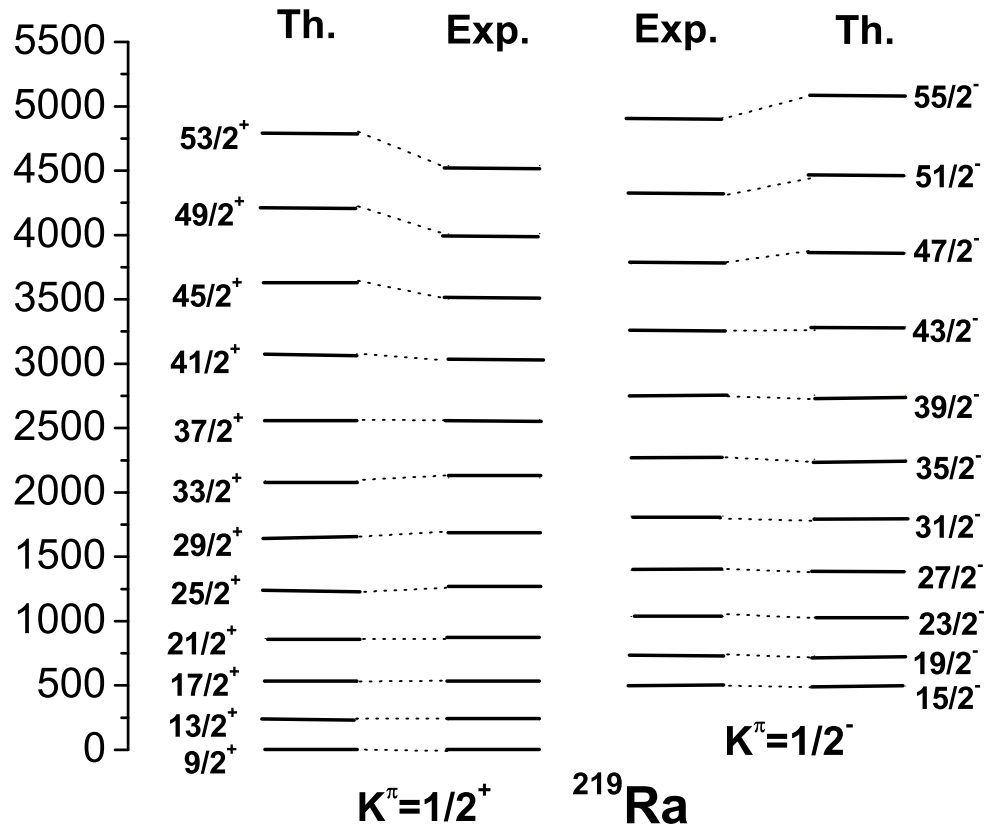

FIG. 16: Calculated (Th.) and experimental(Exp.) excitation energies for the $K^\pi = \frac{1}{2}^\pm$ bands in ^{219}Ra. The data were taken from Ref.[38].

[8, 10] for this nucleus we have $f = 0.8$. The large value of the strength X_3 determines a large mixing amplitudes of the states $[g_{9/2}\Psi_g^{(+)}; f_{5/2}\Psi_g^{(-)}]$ as well as of the states $[g_{9/2}\Psi_g^{(-)}; f_{5/2}\Psi_g^{(+)}]$. Indeed, the value obtained for this amplitude is: $|A_{i,3}^{(+)}|^2 = |A_{1,3}^{(-)}|^2 = 0.07425$. Another distinctive feature for ^{227}Ra consists in the fact that the $\vec{j}\cdot\vec{J}$ interaction strength has a sign which is different from that associated to other nuclei. In fact the repulsive character of this interaction in ^{227}Ra is necessary in order to compensate the large attractive contribution of the q_3Q_3 interaction.

Further, we addressed the question whether one could identify signatures for static octupole de10formation in the two bands. To this goal, in Fig. 18, we plotted the energy displacement functions [10, 11, 31] $\delta E(I), \Delta E_{1,\gamma}(I)$, defined in the previous section, for ^{239}Pu. We choose this nucleus, since more data are available. The plot suggests that a static octupole deformation is

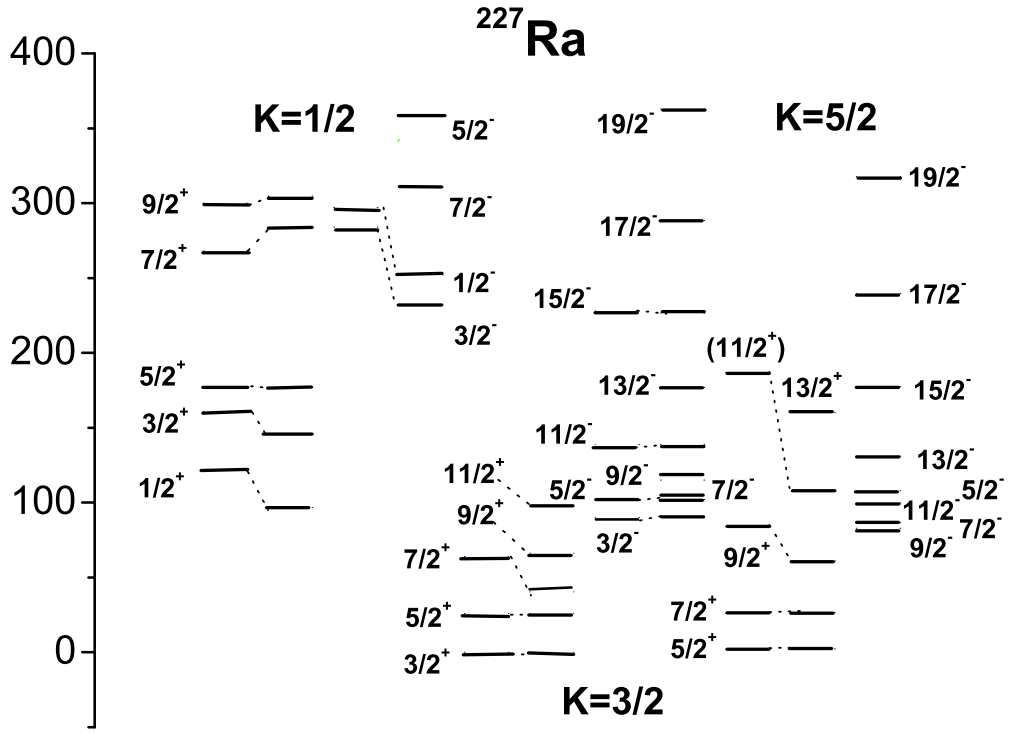

FIG. 17: Calculated and experimental excitation energies for the bands with $K^\pi = \frac{1}{2}^\pm, \frac{3}{2}^\pm, \frac{5}{2}^\pm$ in ^{227}Ra. The experimental data were taken from Refs.[28, 35, 38]

possible for the states with angular momenta $I \geq \frac{51}{2}$ belonging to the two parity partner bands.

Finally we calculated the branching ratio R_J defined by Eq.(3.17), for ^{219}Ra. There are two parameters involved which were fixed so that two particular experimental data are reproduced. The values obtained for these parameters are:

$$\begin{aligned} \text{present}^1: \quad & \frac{q_1}{q_2} = 18.377 \times 10^{-3} fm^{-1}, \;\; ab^2 = -0.63616 fm^2, \\ \text{present}^2: \quad & \frac{q_1}{q_2} = 11.310 \times 10^{-3} fm^{-1}, \;\; ab^2 = -0.34422 fm^2, \end{aligned} \tag{3.20}$$

where b denotes the oscillator strength characterizing the spherical shell model states for the odd nucleon. As shown in Table III, the theoretical results agree resonable well to the corresponding experimental data. Our results show an oscilating behavior with maxima for the negative parity states. Note that some off the data are well described while others deviate from the data by a factor ranging from 2 to 3. In the third column of Table V we listed the results obtained in Ref.[34]

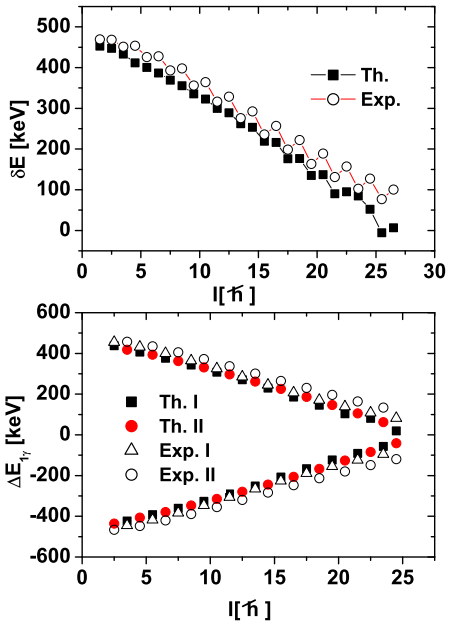

FIG. 18: The theoretical and experimental energy displacement functions $\delta E(I)$ and $\Delta E_{1,\gamma}(I)$ given by Eqs.(2.21) and (2.22) respectively, characterizing the isotope ^{239}Pu, are plotted as a function of the angular momentum I. Experimental data are taken from Ref.[32]. In the lower panel, the theoretical and experimental $\Delta E_{1,\gamma}(I)$ corresponding to the states $I^\pi = \left(\frac{1}{2}+2k\right)^+$ with k=1,2,3,..., are represented by the symbols labeled by $Th.I$ and $Exp.I$ respectively, while those associated with the negative parity states $I^\pi = \left(\frac{1}{2}+2k\right)^-$ with k=1,2,3,... bear the labels $Th.II$ and $Exp.II$, respectively.

by a different model.

IV. CONCLUSIONS

The results presented above may be summarized as follows: States of four pairs of partner bands $g^\pm, \beta^\pm, \gamma^\pm, 1^\pm$, are projected from four orthogonal states having both quadrupole and octupole deformation. The interleaved structure of positive and negative parity states, which have been seen in some nuclei, is well reproduced. The low position for the state 1^- in ^{218}Ra and ^{220}Ra is caused by the $\vec{J}_2\vec{J}_3$ interaction. The back bending of the angular momentum represented as function of the rotational frequency, seen in ^{218}Ra, is nicely reproduced. From the analysis of energy displacement

	$\frac{B(E1;J\rightarrow(J-1))}{B(E2;J\rightarrow(J-2))}[10^{-6}fm^{-2}]$			
$J^\pi - J_{g.s.}$	Exp.	*present*[1]	*present*[2]	Ref.[34]
5^-	2.52(18)	2.52	2.52	1.195
6^+	1.12(08)	1.09	0.677	0.314
7^-	1.49(10)	3.97	3.284	1.318
8^+	1.23(16)	1.23	0.704	0.313
9^-	1.16(08)	4.56	3.194	1.442
10^+	2.77(64)	1.44	0.775	0.312
11^-	1.41(9)	4.59	2.829	1.567
12^+	3.68(26)	1.69	0.868	0.313
13^-	2.14(30)	4.39	2.448	1.691
14^+	1.96(14)	1.96	0.967	0.314
15^-	1.76(18)	4.11	2.131	1.814
16^+	1.06(17)	2.22	1.060	0.315
17^-	2.08(28)	3.84	1.887	1.936
18^+	3.34(48)	2.45	1.137	0.317
19^-	1.34(42)	3.62	1.704	2.057
20^+	2.38(44)	2.63	1.195	0.318
21^-	4.01(94)	3.44	1.568	2.177
Average	2.09(9)	2.97	1.7	1.072

TABLE III: Experimental (Exp.) and calculated values of the ratio $B(E1)/B(E2)$ for the initial state J^π running from $19/2^-$ to $51/2^-$. For an easier writting the angular momenta are normalized to $J_{g.s.} = 9/2$. Experimental data are from Ref.[37]. Results are given in units of $10^{-6}fm^{-2}$. For comparison on the last column we give the results from Ref.[34].

functions (e.d.f.) it results that the settlement of the octupole static deformation in the excited bands, takes place for different angular momenta. Moreover, there are several distinct situations: a) The vanishing of the e.d.f. takes place only for the gb. b) the vanishing takes place in g, β and γ bands but at different angular momenta. c) the vanishing appears in γ band but not in other bands. The jump in the E1 transition probability seen in ^{226}Ra for the $g^\pm$ bands, for the angular momenta were the static octupole deformation is set on, is reproduced. Note that the

octupole deformation causes an electric dipole moment, due to the charge distribution. For the dipole band such a jump is not seen. However, a jump in the M1 transition shows up. We believe that this is a distinctive feature for the dipole bands. The plot of the dynamic moment of inertia indicates that each dipole band is a reunion of two distinct bands. For these bands an interleaved structure with the corresponding bands of opposite parity can be seen. The angle $(\vec{J}_2, \vec{J}_3)$ in the states of $g^{\pm}, \beta^{\pm}, \gamma^{\pm}$ reaches a minimum for a certain J, then is slightly increasing and a saturation is obtained for $\varphi = \pi/2$. By contrast in the dipole bands the angle is a monotone decreasing function of J. Comparing the M1 branching ratios for the bands 1^+ and 1^- one has concluded that the band 1^+ is of magnetic nature. Doing the same with E1 branching ratio one concludes that the band 1^- is of an electric character. The magnetic states from the band 1^+ are different from the so called scissors states. Indeed, they are rather of shares nature. We have seen that there are states where the angle $(\vec{J}_2, \vec{J}_3)$ is $\pi/2$. These states are precursors of a chiral symmetry. This formalism is the only one which treats correctly the rotational degrees of freedom. All the others overestimate the contribution of the Eulerian angles. By contrast to other boson formalisms, where in order to obtain an octupole deformed shape is necessary to have a fourth order octupole boson Hamiltonian, here a second order term is enough to cause a static octupole deformation. Note that all the terms involved in the model Hamiltonian have a microscopic justification within a boson expansion formalism applied to a two body quadrupole-quadrupole plus octupole-octupole interaction [26].

Comparison between our formalism for even-odd nuclei and that of Ref. [36], reveals the following features: i) Having in mind the asymptotic behavior of the coherent states written in the intrinsic frame of reference [14], one may anticipate that the wave function describing the odd system from Ref. [36], might be recovered in the asymptotic limit of the present approach. Due to the fact that our formalism is associated to the laboratory reference frame, the Coriolis interaction does not show up explicitly. The split of the states of different parities is determined by the matrix elements of H_{pc}. ii) Since the coherent states are axially symmetric functions, we don't account for the motion of the γ-like deformation. Again the two formalisms are on a par with each other. iii) The approach of Ref. [36] is of a strong coupling type and therefore K is a good quantum number, which is not the case in our approach. Indeed, we use the laboratory frame and the meaning of the quantum number K is given by the fact that the K-component of the spherical function prevails over the components with $K' \neq K$. iv) The Hamiltonian describing the odd system (3.1) involves a

term H_{core} which describes in a realistic fashion the neighboring even-even system. By contrast, in Ref.[36] the terms associated to the core are not appropriate for describing the complex structure of the even-even sub-system.

Before closing, we would like to add few remarks about the possible development of the present formalism. Choosing for the core unprojected states, the generating states for the parity partner bands with $K^\pi = 0^\pm_\beta, 2^\pm_\gamma, 1^\pm$ states, otherwise keeping the same single particle basis for the odd nucleon, the present formalism can be extended to another four bands, two of positive and two of negative parity. Another noteworthy remark refers to the chiral symmetry [39] for the composite particle and core system. Indeed, in Section III we showed that starting from a certain total angular momentum of the core, the angular momenta carried by the quadrupole ($\vec{J}_2$) and octupole ($\vec{J}_3$) bosons respectively, are perpendicular on each other. Naturally, we may ask ourselves whether there exists a strength for the particle-core interaction such that the angular momentum of the odd particle becomes perpendicular to the plane $(\vec{J}_2, \vec{J}_3)$. This would be a signature that the three component system exhibits a chiral symmetry.

As a final conclusion, one may say that the present CSM extension to odd nuclei can describe quite well the excitation energies in the parity partner bands with $K^\pi = \frac{1}{2}^\pm, \frac{3}{2}^\pm, \frac{5}{2}^\pm$.

Acknowledgment. This paper was supported by the Romanian Ministry of Education and Research , CNCSIS, under the contracts PNII, No. ID-545/2008, cod ID-1038.

---

[1] F. Asaro, F. S. Stephen, I. Perlman, Phys. Rev. **92** (1953) 1495.

[2] F. S. Stephen, Jr., F. Asaro and I. Perlman, Phys. Rev. **100** (1955) 1543.

[3] R. R. Chasman, Phys. Rev. Lett. **42**, 630 (1979); Phys. Lett **B 96**, 7 (1980).

[4] P. Möller and J. R. Nix, Nucl. Phys. **A 361**, 117 (1981).

[5] S. G. Rohozinski, Rep. Prog. Phys. **51**, 541 (1988).

[6] P. A. Butler and W. Nazarewicz, Rev. Mod. Phys. **68**, 349 (1996).

[7] A. A. Raduta, Al. H. Raduta, A. Faessler, Phys. Rev. **C 55**, 1747 (1997).

[8] A. A. Raduta, Al. H. Raduta, A. Faessler, J. Phys. **G 23**, 149 (1997).

[9] A. A. Raduta, A.Faessler, R. K. Sheline, Phys. Rev. **C 57**, 1512 (1998).

[10] A. A. Raduta, D. Ionescu, A. Faessler, Phys. Rev. **C 65**, 064322 (2002).

[11] A.A. Raduta and D. Ionescu, Phys. Rev. **C67**,044312 (2003).

[12] A. A. Raduta, C. M. Raduta, A. Faessler, Phys. Lett. **B 635**, 80 (2006).

[13] A. A. Raduta, C. M. Raduta, Nucl. Phys. **A 768**, 170 (2006).

[14] A. A. Raduta, *et al.*, Phys. Lett. **B99** , 444 (1981); Nucl. Phys. **A 381**, 253 (1982).

[15] R.K.Sheline, Rev. Mod. Phys. **32**, 1 (1960).

[16] M.Sakai, Nucl. Phys. **A104** ; Nucl. Data Tables **10**, 511 (1972).

[17] A.A.Raduta, C. Lima and A. Faessler, Z. Phys. **A313**, 69 (1983).

[18] A.A.Raduta, S.Stoica, Z. Phys. **A327**, 275 (1987).

[19] A. A. Raduta, A. Faessler, V. Ceausescu, Phys. Rev. **36**, 2111 (1987).

[20] A. A. Raduta, N. Lo Iudice and I. I. Ursu, Nucl. Phys. A 608, 11 (1996).

[21] A. A. Raduta, D. Ionescu, I. I. Ursu and A. Faessler, Nucl. Phys. **A720**, 43, (2003).

[22] D. Ionescu, PhD Thesis, IFIN-HH, Bucharest, 2003, unpublished.

[23] P.M.Walker *et al.*, Phys. Lett. **87 B**, 339 (1979).

[24] H. J. Wollershein *et al.*, Nucl. Phys. **A556**, 261 (1993).

[25] N. Lo Iudice and F. Palumbo, Phys. Rev. Lett. **41**, 1532 (1978).

[26] A.A. Raduta et *al.*, Phys. Rev. **C 8**, 1525 (1973).

[27] A. A. Raduta, V. Ceausescu and R. M. Dreizler, Nucl. Phys. **A 272**, 11,(1976).

[28] G. A. Leander, *et al.,* Nucl. Phys. **A 388**, 452, (1982).

[29] A. A. Raduta, C. M. Raduta, A. Faessler, Phys. Rev. C **80** (2009) 044327.

[30] Peter Ring and Peter Schuck, *The Nuclear Many-Body Problem*, Springer-Verlag, Berlin, Heidelberg, New York, 2000, pp. 76.

[31] D. Bonatsos *et al.*, Phys. Rev. **C62**, 024301, (2000).

[32] S. Zhu *et al.*, Phys. Lett. **B 618**, 51, (2005).

[33] A.Ya Dzyublik and V. Yu Denisov, Yad. Fiz. **56**, 30, (1993) [Phys. At. Nucl. **56**, 303 (1993)].

[34] V. Yu. Denisov and A. Ya. Dzyublik, Yad. Fiz.**56**, 96,(1993) [Phys. At. Nucl. **56**, 477 (1993)]

[35] V. Yu Denisov and A.Ya Dzyublik, Nucl. Phys. **A 589**, 17, (1995).

[36] N. Minkov, *et al.,* Phys. Rev. **C76**, 034324, (2007).

[37] P. D. Cottle *et al.* Phys. Rev. **C36** ,2286 (1987).

[38] M. Wieland *et al.*, Phys. Rev. **C 45** 1035 (1992).

[39] S. Frauendorf, J. Meng, Nucl. Phys. **A617**, (1997) 131.